Demonstration of Brain Tumor-Induced Neurovascular Uncoupling in Resting-State fMRI at Ultrahigh Field

Shruti Agarwal,[1] Haris I. Sair,[1] Raag Airan,[1] Jun Hua,[2,3] Craig K. Jones,[2,3] Hye-Young Heo,[2,3] Alessandro Olivi,[4] Martin A. Lindquist,[5] James J. Pekar,[2,3] and Jay J. Pillai[1]

Abstract

To demonstrate in a small case series for the first time the phenomenon of brain tumor-related neurovascular uncoupling (NVU) in resting-state blood oxygen level-dependent (BOLD) functional magnetic resonance imaging (fMRI) at ultrahigh field (7T). Two *de novo* (i.e., untreated) brain tumor patients underwent both BOLD resting-state fMRI (rsfMRI) on a 7T MRI system and motor task-based BOLD fMRI at 3T. Ipsilesional (i.e., ipsilateral to tumor or IL) and contralesional (i.e., contralateral to tumor or CL) region of interest (ROI) analysis was performed on both 3T motor task-related general linear model-derived activation maps and on 7T rsfMRI independent component analysis (ICA)-derived sensorimotor network maps for each case. Asymmetry scores (ASs) were computed based on numbers of suprathreshold voxels in the IL and CL ROIs. In each patient, ASs derived from ROI analysis of suprathreshold voxels in IL and CL ROIs in task-related activation maps and rsfMRI ICA-derived sensorimotor component maps indicate greater number of suprathreshold voxels in contralesional than ipsilesional sensorimotor cortex in both maps. In patient 1, an AS of 0.2 was obtained from the suprathreshold Z-score spectrum (voxels with Z-scores >5.0) of the task-based activation map and AS of 1.0 was obtained from the suprathreshold Z-score spectrum (Z-scores >5.0) of the ICA-derived sensorimotor component map. Similarly, in patient 2, an AS of 1.0 was obtained from the suprathreshold Z-score spectrum (Z-scores >5.0) of the task-based activation map and an AS of 1.0 was obtained from the suprathreshold Z-score spectrum (Z-scores >5.0) of the ICA-derived sensorimotor component map. Overall, decreased BOLD signal was noted in IL compared with CL ROIs on both task-based activation maps and ultrahigh field resting-state maps, indicating the presence of NVU. We have demonstrated evidence of NVU on ultrahigh field 7T rsfMRI comparable with the findings on standard 3T motor task-based fMRI in both cases.

Key words: motor activation; neurovascular uncoupling; presurgical mapping; resting state fMRI; ultra-high field

Introduction

BLOOD OXYGEN LEVEL-DEPENDENT functional magnetic resonance imaging (BOLD fMRI) detects hemodynamic changes (such as changes in blood volume, blood flow, and oxygenation) that occur in response to neuronal activity. Brain activation mapping using BOLD fMRI relies on the fact that hemodynamic changes and neuronal activity are tightly coupled (Attwell et al., 2010; Kim and Ogawa, 2012). However, in patients with brain tumors or other focal brain lesions, the coupling between neuronal activity and the hemodynamic changes occurring in the adjacent vasculature is often disrupted, resulting in false-negative BOLD fMRI activation that can lead to inadvertent eloquent cortical resection and resultant postsurgical permanent disability (Holodny et al., 2000). This phenomenon of neurovascular uncoupling (NVU) is an under-recognized, but critical, limitation of clinical fMRI (Holodny et al., 2000; Hou et al., 2006; Ulmer et al., 2003). Investigations relating to brain tumor-related NVU and its effects on fMRI have been performed to date with task-based fMRI only and at conventional MRI field strengths (3 Tesla and lower) (Holodny

[1]Division of Neuroradiology, Russell H. Morgan Department of Radiology and Radiological Science, Johns Hopkins University School of Medicine, Baltimore, Maryland.
[2]Division of MR Research, Russell H. Morgan Department of Radiology and Radiological Science, Johns Hopkins University School of Medicine, Baltimore, Maryland.
[3]F.M. Kirby Research Center for Functional Brain Imaging, Kennedy Krieger Institute, Baltimore, Maryland.
[4]Department of Neurosurgery, Johns Hopkins University School of Medicine, Baltimore, Maryland.
[5]Department of Biostatistics, Johns Hopkins University Bloomberg School of Public Health, Baltimore, Maryland.

et al., 2000; Hou et al., 2006; Jiang et al. 2010; Ulmer et al., 2003; Zacà et al., 2014). A previous study (Zacà et al., 2014) demonstrated brain tumor-related NVU through a combination of breath hold cerebrovascular reactivity (BH CVR) and task-based fMRI, while another publication (Agarwal et al., 2015) demonstrated tumor-related NVU in resting-state fMRI (rsfMRI). However, neither publication directly compared task-based fMRI with rsfMRI, and both were performed at 3T. Although both studies involved low-grade gliomas with larger patient cohorts, neither explored the effects of NVU on BOLD signal at ultrahigh field.

In the current series, we present two cases that illustrate that the problem of brain tumor-related NVU may also similarly affect rsfMRI at ultrahigh field (7 Tesla), despite known substantial BOLD signal-to-noise ratio advantages for rsfMRI provided by higher field strength, which may not fully mitigate the effects of such NVU.

Materials and Methods

Patients

Two patients with *de novo* primary low-grade perirolandic oligodendroglial tumors referred for routine 3T clinical presurgical fMRI mapping at our institution also underwent a 7T fMRI study on the same day as their 3T fMRI examination.

Patient No. 1. A 36-year-old male patient presented with right perirolandic low-grade oligoastrocytoma (WHO grade II). The lesion expands the right postcentral gyrus with both cortical and subcortical involvement involving the anterior and posterior margins of the right postcentral sulcus. The patient experienced multiple episodes of left facial numbness that have progressively increased in intensity and which occasionally are accompanied by left upper extremity sensory disturbances. This patient demonstrated strong right-handedness with very minimal tendency toward ambidexterity based on his responses on the Edinburgh Handedness Inventory standardized questionnaire (30 right-handed and only 2 left-handed responses).

Patient No. 2. A 23-year-old male patient presented with left frontoparietal opercular low-grade (WHO grade II) oligodendroglioma. He initially presented with tongue numbness and blurry vision, which progressed over a year to sensorimotor seizures involving his right index finger and thumb, at which time he was started on antiepileptic medication. Despite medical therapy, his seizures continued to progress, thus surgical management was considered. This patient demonstrated overall right-handedness with a mild tendency toward ambidexterity based on his responses on the Edinburgh Handedness Inventory questionnaire (22 right-handed and 7 left-handed responses).

Each patient provided signed, written informed consent for participation in this study; the entirety of the study, including content of consent forms, imaging protocol, and subsequent data analysis, was approved by our Institutional Review Board.

MR imaging protocol

Patients underwent clinical fMRI on a 3.0 Tesla (T) MR scanner (Siemens Trio; Siemens Medical Solutions, Erlangen, Germany) equipped with a 12-channel head matrix coil. Three-dimensional (3D) T1-weighted imaging sequence (TR = 2300 msec, TI = 900 msec, TE = 3.5 msec, flip angle = 9°, field of view = 24 cm, acquisition matrix = 256 × 256 × 176, slice thickness = 1 mm), two-dimensional (2D) T2 fluid-attenuated inversion recovery (FLAIR) imaging sequence (TR = 9000 msec, TI = 2500 msec, TE = 116 msec, flip angle = 141°, field of view = 17.2 cm × 23 cm, acquisition matrix = 240 × 320 × 53, slice thickness = 3 mm, slice gap = 3 mm), functional single-shot gradient echo planar imaging T2*-weighted BOLD sequences (TR = 2000 msec, TE = 30 msec, flip angle = 90°, field of view = 24-cm, acquisition matrix = 64 × 64 × 33, slice thickness = 4 mm, slice gap = 1 mm).

A 3-min duration vertical tongue movement (TM) task was used for task-based fMRI, consisting of three cycles of 30-sec blocks of rest, followed by 30-sec blocks of repetitive vertical TM.

Each patient underwent training in a session outside the scanner to make sure that tasks could be correctly performed. Real-time fMRI was used to monitor patient task performance. Based on both prescan training (observation of performance outside the MRI scanner) and actual monitoring of task performance inside the scanner (based on real-time fMRI mapping), as well as self-report of patient performance after completion of each task, the patients demonstrated excellent task performance on the reported TM tasks. No tongue weakness or lateral tongue deviation was noted in either patient, and no facial asymmetry was present. Furthermore, no hand/arm weakness was present in either case. Although not included in the figures in this article, hand representation area (RA) activation within the primary motor cortex was preserved bilaterally as well, and both patients were able to perform finger tapping hand motor tasks well based on actual observation through an LCD monitor in the MRI scanner console room.

Neither patient exhibited substantial motor neurological deficit that would be indicative of tumor-related destruction of eloquent cortex, and neither patient experienced any difficulty performing the tasks, but both patients demonstrated abnormally decreased motor task-related activation in the face RA of the primary sensorimotor cortex in the ipsilesional (i.e., ipsilateral to the tumor) hemisphere. Such findings were indicative of NVU in the absence of corresponding substantial neurological (i.e., motor) deficit.

7T scanning was performed using research sequences on a 7.0T Philips MRI system equipped with a 32-channel head matrix coil. Imaging protocol included a 3D T1 3D MPRAGE imaging sequence (TR = 4.023 msec, TE = 1.81 msec, flip angle = 7°, field of view = 22 cm, acquisition matrix = 224 × 224 × 180, slice thickness = 1 mm) for structural imaging and multiple 2D fast echo planar imaging T2*-weighted BOLD sequences for resting-state functional imaging (TR = 2500 msec, TE = 22 msec, flip angle = 80°, field of view = 19.2 cm, acquisition matrix = 128 × 128 × 31, slice thickness = 3 mm). The BOLD parallel imaging acceleration (SENSE) factor = 3.

For rsfMRI, 140 volumes were acquired, and each patient was instructed to remain still with eyes closed during the entire acquisition.

Data analysis

3T task-based fMRI data were processed using analysis of functional neuroimages (Cox, 1996) software. Preprocessing

of EPI data included slice-timing correction, spatial realignment to correct for head motion, and spatial smoothing with a 3D Gaussian kernel with a full width at half maximum (FWHM) of 6 mm. A standard general linear model analysis was performed using AFNI to obtain standard task-based activation T-value maps. Z-scores were then calculated from the obtained T-value maps.

7T rsfMRI data were corrected for slice time and spatial realignment, followed by nuisance regression using anatomical component-based noise correction (aCompCor) per Behzadi and associates (2007), scrubbing of outlier volumes detected by the ART repair toolbox (Mazaika et al., 2009), band-pass filtering at 0.1–0.01 Hz, and smoothing with a 6-mm FWHM Gaussian kernel. Independent component analysis (ICA) with 35 target components was subsequently performed using the GIFT toolbox (Correa et al., 2005) utilizing the Infomax algorithm with ICASSO to determine the reliability of ICA results (Himberg and Hyvarinen, 2003). Three experienced raters (J.J.P., S.A., and H.I.S.) visually inspected all 35 ICA-derived components in each case. In each case, the sensorimotor component selection was made through consensus among the raters; the selected component displays BOLD signal change within the anatomic precentral and postcentral gyri. The raters include two subspecialty board-certified neuroradiologists with specific expertise in functional neuroimaging as well as an imaging scientist with 5 years of postdoctoral neuroimaging experience.

3T and 7T data volumes of each patient were coregistered to the patient's 3T T2 FLAIR images using the automatic affine image registration method provided in the MIPAV software package (http://mipav.cit.nih.gov). Regions of interest (ROIs) were drawn on the ipsilesional (i.e., ipsilateral to the tumor) hemisphere (IL ROI) in consecutive axial sections in z-axis along the entire lesion volume contouring the lesions and extended up to two gyri anterior and posterior to the lesion margins to include perilesional as well as intralesional BOLD signal changes. Each ROI was mirrored on the contralesional (i.e., contralateral to the tumor) hemisphere (CL ROI).

To quantitatively assess the degree of asymmetry of the 3T motor task maps and 7T rsfMRI maps, we utilized a technique similar to the well-documented laterality index used for hemispheric language lateralization (Desmond et al., 1995). We defined an asymmetry score (AS) as [contralesional − ipsilesional active voxels]/[contralesional + ipsilesional active voxels]. Similar to standard laterality indices, positive AS indicates greater numbers of active voxels in the contralesional ROIs compared with the ipsilesional ROIs.

Results

Figure 1 displays the ROI analysis and Z-score spectrum for Patient No. 1. The first row shows a few slices of the suprathreshold 3T BOLD activation map (displaying voxels above a threshold of 5.0 Z-score in the expected face RA of the primary sensorimotor cortex in red) overlaid on structural T2 FLAIR images during performance of a vertical TM fMRI task at 3T. The manually drawn ipsilesional (IL) ROI was mirrored to obtain the contralesional (CL) ROI (white contours). The IL ROI includes the entire tumor and up to two gyri anterior and posterior to the lesion margins. Such 2D ROIs were manually delineated in all consecutive axial sections where lesion as well as in-plane contralesional
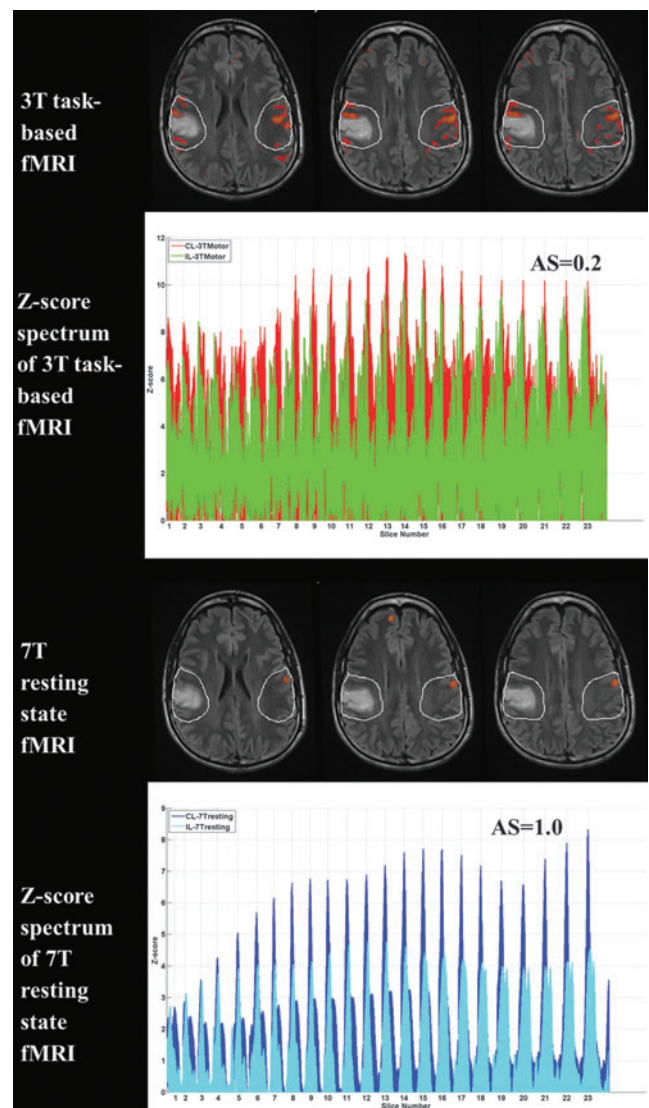

FIG. 1. Demonstration of NVU on both 3T task-based sensorimotor activation map and 7T BOLD resting-state ICA-derived sensorimotor component map in Patient No. 1 with a right perirolandic low-grade oligoastrocytoma (grade II). The 3T tongue motor task fMRI (first row) and 7T rsfMRI (third row) maps were overlaid on T2 FLAIR images with IL ROI and CL ROI shown in white contours with suprathreshold voxels displayed in red. The second and fourth rows demonstrate the Z-score spectra of voxels within IL and CL ROIs in the 3T motor fMRI task and 7T rsfMRI maps, respectively. BOLD, blood oxygen level-dependent; CL, contralesional; FLAIR, fluid-attenuated inversion recovery; fMRI, functional magnetic resonance imaging; ICA, independent component analysis; IL, ipsilesional; NVU, neurovascular uncoupling; ROI, region of interest; rsfMRI, resting-state fMRI.

activation was present. The second row displays the Z-score spectrum of voxels within IL and CL ROIs in all such slices of the task-based activation map. An asymmetry (i.e., laterality) score (AS) of 0.2 was obtained from the suprathreshold Z-score spectrum (voxels with Z-scores greater than 5.0). Similarly, the third row shows a few slices of the suprathreshold 7T BOLD resting-state maps of the same patient displaying the ICA-derived sensorimotor component (red

voxels with *Z*-score >5.0) overlaid on structural T2 FLAIR images along with IL and CL ROIs (white contours). The *Z*-score spectrum of voxels within these IL and CL ROIs along consecutive slices is displayed in the fourth row. An AS of 1.0 was obtained from the suprathreshold *Z*-score spectrum (voxels with *Z*-scores greater than 5.0). Please note that this is a case of moderate NVU, as reflected in the task-based fMRI AS of 0.2.

Figure 2 displays the ROI analysis and *Z*-score spectrum for Patient No. 2. The first row shows a few slices of the suprathreshold 3T BOLD activation map (displaying voxels
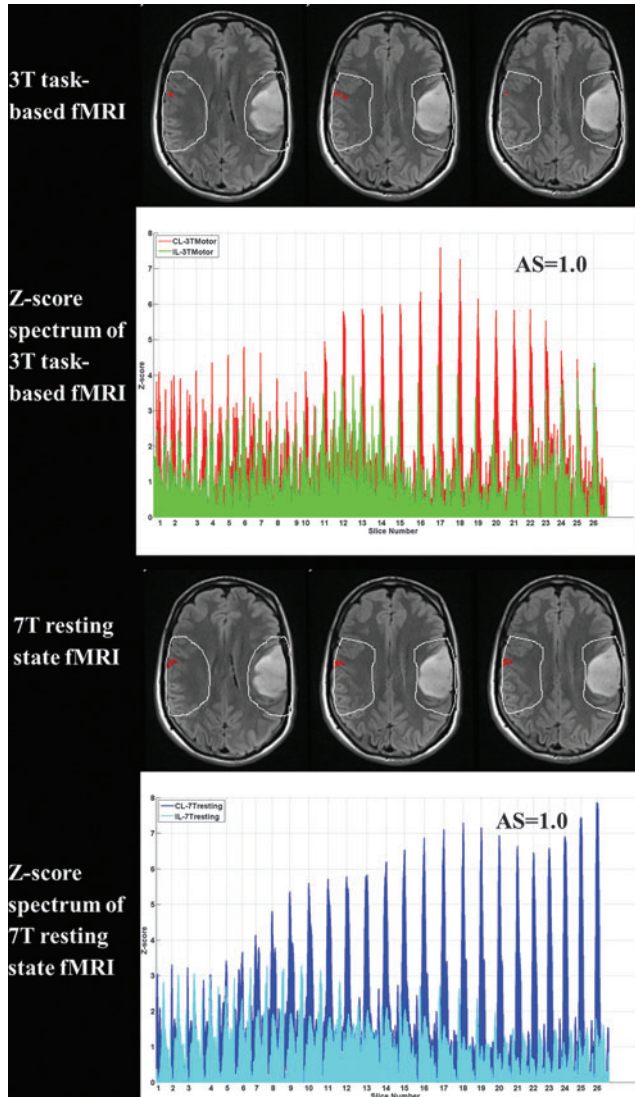
above a threshold of 5.0 *Z*-score in the expected face RA of the primary sensorimotor cortex in red) overlaid on structural T2 FLAIR images during performance of a vertical TM fMRI task at 3T. The manually drawn ipsilesional (IL) ROI was mirrored to obtain the contralesional (CL) ROI (white contours). IL ROI includes the entire tumor and up to two gyri anterior and posterior to the lesion margins. Such 2D ROIs were manually delineated in all consecutive axial sections where lesion as well as in-plane contralesional activation was present. The second row displays the *Z*-score spectrum of voxels within IL and CL ROIs in all such slices of task-based activation map. An asymmetry (i.e., laterality) score (AS) of 1.0 was obtained from the suprathreshold *Z*-score spectrum (voxels with *Z*-scores greater than 5.0). Similarly, the third row shows a few slices of the suprathreshold 7T BOLD resting-state maps of the same patient displaying the ICA-derived sensorimotor component (red voxels with *Z*-score >5.0) overlaid on structural T2 FLAIR images along with IL and CL ROIs (white contours). The *Z*-score spectrum of voxels within these IL and CL ROIs along the consecutive slices is displayed in the fourth row. An AS of 1.0 was obtained from the suprathreshold *Z*-score spectrum (voxels with *Z*-scores greater than 5.0). Please note that this is a case of severe NVU, as reflected in the AS of 1.0 for both task fMRI and rsfMRI.

Decreased ipsilesional motor task-related activation in the expected face RA of the right primary sensorimotor cortex corresponds to decreased synchronized ipsilesional BOLD signal fluctuations in the resting-state sensorimotor network within the same cortical region in both patients. The asymmetry (i.e., laterality) scores derived from both the 3T motor task and 7T resting-state maps indicate greater numbers of suprathreshold voxels in CL compared with IL ROIs in both maps for each patient. These findings of reduced ipsilesional BOLD signal change in the absence of profound corresponding neurological deficits suggest the presence of NVU in both cases, with the severity of the NVU being greater in Patient No. 2.

FIG. 2. Demonstration of NVU on 3T task-based sensorimotor activation map and 7T BOLD resting-state ICA-derived sensorimotor component map in Patient No. 2 with a left frontoparietal opercular low-grade oligodendroglioma (grade II). The 3T tongue motor task fMRI (first row) and 7T rsfMRI (third row) maps were overlaid on T2 FLAIR images with IL ROI and CL ROI shown in white contours with suprathreshold voxels displayed in red. The second and fourth rows demonstrate the *Z*-score spectra of voxels within IL and CL ROIs in the 3T motor fMRI task and 7T rsfMRI maps, respectively.

Discussion

In both of the presented cases, ipsilesional abnormal decrease in detectable BOLD signal was present relative to normal contralesional BOLD signal in both 7T rsfMRI maps and 3T motor task activation maps. In both cases, these results were reflected in positive ASs for both resting-state and task-based fMRI maps.

Absent or pathologically decreased task-based BOLD fMRI activation in the presence of a tumor or other resectable focal brain lesion, in the absence of a focal neurological deficit attributable to destruction of the eloquent cortical region that would be expected to produce a robust BOLD response, represents direct evidence of NVU (Hou et al., 2006; Ulmer et al., 2003; Zacà et al., 2014). Although some degree of asymmetry of task-based activation in the primary motor network has been reported in previous studies of normal volunteers (Dassonville et al., 1997; Jancke et al., 1998; Solodkin et al., 2001), the degree of asymmetry observed has been less substantial than what we observed in patients with gliomas, both in this small series and in prior publications that included larger patient series (Agarwal et al., 2015; Zacà et al., 2014). For this reason,

we chose to rely solely on such task-based motor activation maps to establish the presence of NVU in these two patients with brain tumors in proximity to eloquent motor cortex. To our knowledge, our current study is the first demonstration of NVU in brain tumors using ultrahigh field rsfMRI data.

Compared with task-based fMRI, rsfMRI has potential advantages in presurgical mapping and other clinical applications, including the need for compliance only with respect to avoidance of head motion rather than active cognitive task performance, as well as the absence of need for specialized stimulus presentation hardware and software. rsfMRI may thus be performed for presurgical mapping in some patients who may not be candidates for task-based fMRI (Fukunaga et al., 2006; Kiviniemi et al., 2003; Kokkonen et al., 2009; Liu et al., 2009; Peltier et al., 2005; Shimony et al., 2009). Several articles have recently been published suggesting that there may be potential advantages of using resting-state BOLD fMRI as a preoperative mapping tool. For example, Zhang and associates (2009) compared resting-state functional connectivity to task-based fMRI in patient candidates for brain surgery with tumors near the sensorimotor cortex and demonstrated the ability of resting-state functional connectivity to localize sensorimotor areas using a seed-based approach. Kokkonen and associates (2005) illustrated the convergence between ICA analysis of rsfMRI and task-based fMRI in identifying sensorimotor areas in patients with tumors. Rosazza and associates (2014) assessed quantitatively the degree of correspondence between multiple rsfMRI analyses (ICA and seed-based approaches) and task-based fMRI in the context of presurgical mapping of motor functions to localize the hand, foot, and mouth motor areas in a group of patients with lesions close to the primary sensorimotor cortex.

While ICA is a completely data-driven analysis, ROI-based or seed-based approaches rely on prior anatomic hypotheses to restrict the analysis to a predefined set of ROIs or to a specific seed region. Joel and associates (2011) have reported the strengths and weaknesses of each method. ICA can automatically isolate sources of noise; however, the decomposition results vary depending on the choice of the number of components (Remes et al., 2010). ROI-based analysis results are relatively straightforward; however, it is based on *a priori* anatomic hypotheses (and thus may be inaccurate in cases of aberrant functional anatomy), and nonneuronal fluctuations can bias the observed correlations (Fox and Raichle, 2007). We chose to perform ICA since it represents a data-driven (i.e., unsupervised) approach to rsfMRI analysis.

In previous studies, task-based motor fMRI activation maps were used to validate BH CVR maps as an effective method for the assessment of NVU in low-grade perirolandic tumors (Zacà et al., 2014). In that study, the results of analyzed ipsilesional and contralesional ROIs demonstrated significant ipsilesional decreases in both mean task-based motor activation T values and mean BH CVR T values indicative of NVU as patients did not exhibit clinical deficits precluding their performance of the corresponding tasks. In our current case series, the patients did undergo BH CVR mapping, and the BH CVR maps did display concordant ipsilesional decreases in CVR that correspond to tumor-induced NVU. For the purpose of our current study, we performed comparison of ipsilesional with contralesional results of both task-based motor fMRI activation and rsfMRI analysis for the demonstration of NVU in rsfMRI. In this illustrative series, we performed single-subject level analysis using AS comparing IL and CL ROIs in individual cases.

In this small sample of two low-grade glioma cases, the exact pathophysiologic mechanism for the suspected NVU is not clear. Although electrochemical disruptions of the normal neurovascular coupling cascade at the neurotransmitter or postsynaptic chemical mediator level may be contributory, astrocytic dysfunction related to tumor infiltration of eloquent sensorimotor cortex may also contribute to the ipsilesional decrease in observed task and resting-state BOLD signal (Agarwal et al., 2015; Attwell et al., 2010; Zaca et al., 2014).

Conclusion

In conclusion, despite the limitation of small sample size, these two brain tumor cases illustrate for the first time at ultrahigh field that NVU affects BOLD signal detectability on both resting-state and task-based fMRI. Astrocytic dysfunction related to tumor infiltration of eloquent cortex may be a contributing factor to our findings that are suggestive of NVU.

Acknowledgments

Author Disclosure Statement

No competing financial interests exist.

References

Agarwal S, Sair HI, Yahyavi-Firouz-Abadi N, Airan R, Pillai JJ. 2015. Neurovascular uncoupling in resting state fMRI demonstrated in patients with primary brain gliomas. J Magn Reson Imaging [Epub ahead of print]; DOI: 10.1002/jmri.25012

Attwell D, Buchan AM, Charpak S, Lauritzen M, Macvicar BA, Newman EA. 2010. Glial and neuronal control of brain blood flow. Nature 468:232–243.

Behzadi Y, Restom K, Liau J, Liu TT. 2007. A component based noise correction method (CompCor) for BOLD and perfusion based fMRI. Neuroimage 37:90–101.

Correa N, Adali T, Li YO, Calhoun VD. Comparison of Blind Source Separation Algorithms for fMRI Using a New Matlab Toolbox: GIFT. In Proceedings of the IEEE Conference on Acoustics, Speech, and Signal Processing (ICASSP), Philadelphia, PA, USA, 2005, pp. 401–404.

Cox RW. 1996. AFNI: software for analysis and visualization of functional magnetic resonance neuroimages. Comput Biomed Res 29:162–173.

Dassonville P, Zhu XH, Uurbil K, Kim SG, Ashe J. 1997. Functional activation in motor cortex reflects the direction and the degree of handedness. Proc Natl Acad Sci U S A 94:14015–14018.

Desmond JE, Sum JM, Wagner AD, Demb JB, Shear PK, Glover GH, et al. 1995. Functional MRI measurement of language lateralization in Wada-tested patients. Brain 118: 1411–1419.

Fox MD, Raichle ME. 2007. Spontaneous fluctuations in brain activity observed with functional magnetic resonance imaging. Nat Rev Neurosci 8:700–711.

Fukunaga M, Horovitz SG, van Gelderen P, de Zwart JA, Jansma JM, Ikonomidou VN, et al. 2006. Large-amplitude, spatially correlated fluctuations in BOLD fMRI signals during extended rest and early sleep stages. Magn Reson Imaging 24:979–992.

Himberg J, Hyvarinen A. ICASSO: Software for Investigating the Reliability of ICA Estimates by Clustering and Visualization. In Proceedings of the IEEE 13th workshop on Neural Networks for Signal Processing (NNSP), Toulouse, France, 2003.

Holodny AI, Schulder M, Liu WC, Wolko J, Maldjian JA, Kalnin AJ. 2000. The effect of brain tumors on BOLD functional MR imaging activation in the adjacent motor cortex: implications for image-guided neurosurgery. AJNR Am J Neuroradiol 21:1415–1422.

Hou BL, Bradbury M, Peck KK, Petrovich NM, Gutin PH, Holodny AI. 2006. Effect of brain tumor neovasculature defined by rCBV on BOLD fMRI activation volume in the primary motor cortex. Neuroimage 32:489–497.

Jancke L, Peters M, Schlaug G, Posse S, Steinmetz H, Muller-Gartner H. 1998. Differential magnetic resonance signal change in human sensorimotor cortex to finger movements of different rate of the dominant and subdominant hand. Brain Res Cogn Brain Res 6:279–284.

Jiang Z, Krainik A, David O, Salon C, Troprès I, Hoffmann D, et al. 2010. Impaired fMRI activation in patients with primary brain tumors. NeuroImage 52:538–548.

Joel SE, Caffo BS, Van Sijl PCM, Pekar JJ. 2011. On the relationship between seed-based and ICA-based measures of functional connectivity. Magn Reson Med 66:644–657.

Kim SG, Ogawa S. 2012. Biophysical and physiological origins of blood oxygenation level-dependent fMRI signals. J Cereb Blood Flow Metab 32:1188–1206.

Kiviniemi V, Kantola JH, Jauhiainen J, Hyvärinen A, Tervonen O. 2003. Independent component analysis of nondeterministic fMRI signal sources. Neuroimage 19:253–260.

Kokkonen SM, Kiviniemi V, Mäkiranta M, Yrjänä S, Koivukangas J, Tervonen O. 2005. Effect of brain surgery on auditory and motor cortex activation: a preliminary functional magnetic resonance imaging study. Neurosurgery 57:249–256.

Kokkonen SM, Nikkinen J, Remes J, Kantola J, Starck T, Haapea M, et al. 2009. Preoperative localization of the sensorimotor area using independent component analysis of resting-state fMRI. Magn Reson Imaging 27:733–740.

Liu H, Buckner RL, Talukdar T, Tanaka N, Madsen JR, Stufflebeam SM. 2009. Task-free presurgical mapping using functional magnetic resonance imaging intrinsic activity. J Neurosurg 111:746–754.

Mazaika PK, Hoeft F, Glover GH, Reiss AL. 2009. Methods and software for fMRI analysis for clinical subjects. Human Brain Mapping 47 Suppl 1:S58.

Peltier SJ, Kerssens C, Hamann SB, Sebel PS, Byas-Smith M, Hu X. 2005. Functional connectivity changes with concentration of sevoflurane anesthesia. Neuroreport 16:285–288.

Remes JJ, Starck T, Nikkinen J, Ollila E, Beckmann CF, Tervonen O, et al. 2010. Effects of repeatability measures on results of fMRI sICA: a study on simulated and real resting-state effects. Neuroimage 56:554–569.

Rosazza C, Aquino D, D'Incerti L, Cordella R, Andronache A, Zacà D, et al. 2014. Preoperative mapping of the sensorimotor cortex: comparative assessment of task-based and resting-state fMRI. PLoS One 9:1–19.

Shimony JS, Zhang D, Johnston JM, Fox MD, Roy A, Leuthardt EC. 2009. Resting-state spontaneous fluctuations in brain activity: a new paradigm for presurgical planning using fMRI. Acad Radiol 16:578–583.

Solodkin A, Hlustik P, Noll DC, Small SL. 2001. Lateralization of motor circuits and handedness during finger movements. Eur J Neurol 8:425–434.

Ulmer JL, Krouwer HG, Mueller WM, Ugurel MS, Kocak M, Mark LP. 2003. Pseudo-reorganization of language cortical function at fMR imaging: a consequence of tumor-induced neurovascular uncoupling. AJNR Am J Neuroradiol 24: 213–217.

Zacà D, Jovicich J, Nadar SR, Voyvodic JT, Pillai JJ. 2014. Cerebrovascular reactivity mapping in patients with low grade gliomas undergoing presurgical sensorimotor mapping with BOLD fMRI. J Magn Reson Imaging 40:383–390.

Zhang D, Johnston JM, Fox MD, Leuthardt EC, Grubb RL, Chicoine MR, et al. 2009. Preoperative sensorimotor mapping in brain tumor patients using spontaneous fluctuations in neuronal activity imaged with functional magnetic resonance imaging: initial experience. Neurosurgery 65:226–236.

Address correspondence to:
Jay J. Pillai
Division of Neuroradiology
Russell H. Morgan Department
of Radiology and Radiological Science
The Johns Hopkins Hospital
Phipps B-100, 1800 Orleans Street
Baltimore, MD 21287

E-mail: jpillai1@jhmi.edu